ÉCOLE POLYTECHNIQUE
FÉDÉRALE DE LAUSANNE

2005-18

LESO-PB

Tracer gas measurement of airflow rates in rooms with several air-handling units and large recirculation rates

Roulet C.-A and al.

Submitted to : International Journal of HVAC & Research

2005, August

TRACER GAS MEASUREMENT OF AIRFLOW RATES IN ROOMS WITH SEVERAL AIR-HANDLING UNITS AND LARGE RECIRCULATION RATES

Roulet C.-A.[1], *Zuraimi M. S.*[2], *Sekhar S. C.*[2] *and Tham K.W*[2]

[1] School of Architecture, Civil and Environmental Engineering, Ecole Polytechnique Fédérale, Lausanne, Switzerland.

[2] Dept. of Building, National University of Singapore, Singapore

ABSTRACT

Methods to measure airflow rates using tracer gas in single air handling units are well known. In some buildings however, in particular in Singapore, rooms are often ventilated with two or more units and present large recirculation rates. Large recirculation ratio homogenise the concentrations, so concentrations in supply and extract ducts are close to each other. In addition, these spaces often present a large time constant, so much time is needed to reach steady state. An adapted methodology to measure not only the airflow rates provided by each unit, but also the inter-units airflow rates and the global ventilation efficiency is presented, together with an example of measurement in an actual building. It is shown that the most accurate method is not the same for small and large recirculation ratios.

INDEX TERMS

Air distribution; commissioning, diagnostics, measurement technique, tracer gas, ventilation rate

NOMENCLATURE

Symbol	Definition	Unit
AHU	air handling unit	
C_{ik}	volume concentration of tracer k at node i	-
f	dummy function	
I_k	injection rate of tracer gas k	m^3/s
k	type of tracer gase	-
P	probability	-
Q_{ij}	airflow rate from node i to node j	m^3/s
R	recirculation rate = recirculated flow rate divided by supply airflow rate	-
RMSE	root mean square error	
t	time	s
$T(P, \nu)$	student coefficient for probability P and degree of freedom ν	-
V	volume	m^3
x	dummy variable	
δC	half confidence interval of concentration	-
δI	half confidence interval of tracer gas injection rate	
δQ	half confidence interval of airflow rate	
δR	half confidence interval of recirculation rate	-
γ	infiltration ratio= infiltration flow rate divided by the supply flow rate	-
ν	degree of freedom	-
τ_n	nominal time constant	s

Symbol	Subscript for:	Symbol	Subscript for:
A, B	air handling units A and B	*r*	return air
e	exfiltration air	*s*	supply air
i	infiltration air	*t*	theoretical
o	outdoor air	*x*	extract air

1 INTRODUCTION

The heating, ventilation and air-conditioning (HVAC) system plays an important role in control of the indoor environment of the building. Studies have reported that any deficiency in the system will affect the thermal comfort and air quality in the occupied space (Fanger, 1997; Simons & Walters, 1998). It is thus essential for the HVAC system to operate efficiently and deliver sufficient conditioned air to the occupants in the building. These include proper balancing of airflow within the distribution system to meet design quantities and measurement of actual airflow rates in the system to be compared with design quantities.

In the balancing of the air distribution system, measurements of airflow are usually performed using the traditional instrumentations such as vane anemometers and pitot-static tubes (ASHRAE, 1999; CIBSE, 1971). However, other popular method to measure airflow rates includes using tracer gas and has been adopted since several decades (ASTM 1988; Presser and Becker 1988; Roulet and L.Vandaele 1991). They are, among other uses, applied for measuring outdoor airflow rates or all the airflow rates occurring in single air handling units (Roulet, Foradini et al. 1994).

The principle is to inject tracer gases in the inlet, supply and/or extract ducts at a known rate, I_k, to measure their equilibrium (steady state) concentrations, C_{ik}, at several carefully chosen locations, and to use the air and tracer gas conservation equation to interpret the measurements and get all required airflow rates Q_{ij} (Figure 1).

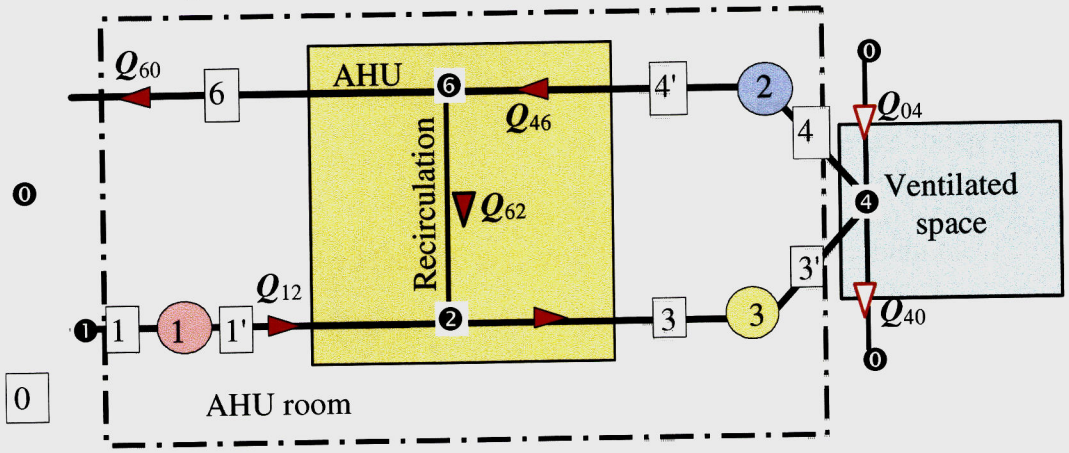

Figure 1: The simplified network representing the air handling unit (AHU) and ducts. Numbers into black circles represent the nodes of the network. Circles are tracer gas injection locations, and numbered rectangles are air sampling locations. Arrows represent possible airflow rates Q_{ij} from node i to nodte j.

In some buildings however, in particular in Singapore, rooms are often ventilated with two or more AHUs. An adapted methodology that could be used to measure not only the airflow rates provided by each AHU, but also to determine the inter-AHUs airflow rates and the global ventilation efficiency is required. The well known tracer gas multizone methodology could be applied in this case. There are however many possibilities in the choice of the

locations for tracer gas injection and air sampling, which lead to many possible systems of equations to interpret the measurements. Among these systems, some are more robust and give more accurate results than others.

Most methods are designed to measure AHUs with recirculation ratios below 50%. This is the case of the method proposed (Roulet, Deschamps et al. 2000), together with an interpretation software. However, air-handling units designed to condition (heat or cool) spaces with large loads such as those found in cold or tropical climates often present large recirculation ratios that homogenise the concentrations, and large nominal time constant (ratio of the ventilated volume to the outdoor airflow rate) that strongly increase the time needed to reach steady state. Among the several possible methods to assess airflow rates, some are better adapted to large recirculation ratios than others.

Therefore, this paper presents a selected method for measuring airflow rates in buildings with two air handling units that serve a single space together, as well as ways to improve the accuracy of tracer gas measurements in systems with high recirculation ratio and large time constant. A case study of an actual measurement is given as an example of application.

2 THEORETICAL BASIS

2.1 Unsteady State and Assessment of Concentrations under Large Recirculation

Using constant injection technique, steady state is quickly reached within ducts, where the air velocity is 1 m/s or more. The concentration difference between air sampled downstream (far enough to get complete mixing) and upstream the tracer gas injection port becomes quickly constant. However, due to the high recirculation, it may take a long time to reach steady state concentrations in the supply duct (location 3) and in the room (location 4), where the air from the room is progressively mixed with outdoor air.

Writing the conservation equation of tracer gas 3 at node 4, in the ventilated space, gives:

$$V\frac{\partial C_{43}}{\partial t} = I_3 + Q_{24}C_{23} + Q_{04}C_{03} - (Q_{46} + Q_{40})C_{43} \qquad (1)$$

Because of the large recirculation ratio, it can be assumed that the concentration is homogeneous in the ventilated space. Dividing this equation by the supply airflow rate Q_{24} gives:

$$\frac{V}{Q_{24}}\frac{\partial C_{43}}{\partial t} = \frac{I_3}{Q_{24}} + C_{23} + \gamma_i C_{03} - (1+\gamma_i)C_{43} \qquad (2)$$

where γ_i is the infiltration ratio Q_{04}/Q_{24}. Using the definition of the nominal time constant τ_n, of the recirculation ratio R, and using the tracer gas conservation at node 2:

$$\frac{V}{Q_{24}} = \frac{V}{Q_{01}}\frac{Q_{01}}{Q_{24}} = \tau_n(1-R) \qquad \text{and} \qquad C_{23} = RC_{43} + (1-R)C_{03} \qquad (3)$$

we get

$$\tau_n(1-R)\frac{\partial C_{43}}{\partial t} = \frac{I_3}{Q_{24}} - (1-R+\gamma_i)(C_{43} - C_{03}) \qquad (4)$$

The steady state concentration is:

$$C_{43}^{\infty} = \frac{I_3}{Q_{34}(1-R+\gamma_i)} + C_{03} \tag{5}$$

and $$C_{43}(t) = C_{43}^{\infty}\left(1-e^{-\frac{t}{\tau}}\right) \qquad \text{with} \qquad \tau = \frac{\tau_n(1-R)}{1-R+\gamma_i} \tag{6}$$

The theoretical exponential can be fitted on the experimental points, allowing the determination of the steady state concentration and time constant without waiting for the equilibrium.

2.2 Determination of Airflow rates

2.2.1 Assessment of airflow rates from measurements

In the method shortly presented in (Roulet and L.Vandaele 1991), it is recommended to inject the tracer gases in the outdoor and extract air ducts (locations 1 and 2 in Figure 1). Air sampling for tracer gas analysis concentration should be taken where complete mixing is achieved, i.e. up to 25 diameters in straight ducts, but less than 3 diameters downstream bends, fans, heat exchangers, etc. In case of mixing problems, tracer could be injected at several places in the same duct section. Supply and extract airflow rates are determined by the following relations (notations according to Figure 1).

The airflow rates, calculated from air and tracer gas mass conservation equations are (I_k is the injection rate of tracer k, and C_{jk} is the steady state concentration of tracer k at location j):

Intake airflow rate $$Q_{12} = \frac{I_1}{C_{1'1} - C_{11}} \tag{7}$$

Supply airflow rate, assuming that the air-handling unit is airtight (tracer k = 2 recommended):

$$Q_{24} = Q_{12}\frac{C_{6k} - C_{1k}}{C_{6k} - C_{3k}} \tag{8}$$

Extract airflow rate $$Q_{46} = \frac{I_2}{C_{62} - C_{42}} \tag{9}$$

Recirculation flow rate $$Q_{62} = Q_{12}\frac{C_{3k} - C_{1k}}{C_{6k} - C_{3k}} \tag{10}$$

Or alternatively $$Q_{62} = Q_{24}\frac{C_{3k} - C_{1k}}{C_{6k} - C_{1k}} \tag{11}$$

Another alternative is to calculate Q_{62} from the recirculation ratio R, if R is assessed using equation (33):

$$Q_{62} = R\,Q_{24} \tag{12}$$

Infiltration flow rate (with $k \neq 3$, recommended value: k= 1):

$$Q_{04} \cong Q_{24}\frac{(C_{3'k} - C_{4k})}{(C_{4k} - C_{0k})} = Q_{12}\frac{(C_{6k} - C_{1k})}{(C_{6k} - C_{3k})}\frac{(C_{3'k} - C_{4k})}{(C_{4k} - C_{0k})} \tag{13}$$

Exfiltration flow rate $$Q_{40} = Q_{04} + Q_{24} - Q_{46} \tag{14}$$

Exhaust airflow rate $$Q_{60} = Q_{04} - Q_{40} + Q_{01} \quad (15)$$

2.2.2 Error analysis of airflow rates

The error analysis is based on the assumption that random and independent errors soil the measurements of tracer gas concentration and injection rates. In this case, the confidence interval of any result, for example an airflow rate, is:

$$[Q - \delta Q; Q + \delta Q] \quad \text{with} \quad \delta Q(x_i) = T(P,\infty)\sqrt{\sum_i \left(\frac{\partial Q}{\partial x_i}\right)^2 \delta x_i^2} \quad (16)$$

where:

$T(P, \infty)$ is the Student coefficient for having the actual value within the confidence interval with probability 1-P

x_i is any variable on which the airflow rate Q depends.

δx_i is the standard deviation of the variable x_i, assumed to be a random variable of mean x_i and normal distribution.

The confidence intervals of the airflow rates are then:

Intake airflow rate $$\delta Q_{12} = T(P,\infty)\sqrt{\frac{(C_{1'1} - C_{11})^2 \delta I_1^2 + I_1^2(\delta C_{1'1}^2 + \delta C_{11}^2)}{(C_{1'1} - C_{11})^4}} \quad (17)$$

Supply airflow rate $$\delta Q_{24} = \sqrt{\delta Q_{12}^2 + \delta Q_{62}^2} = \frac{T(P,\infty)}{(C_{6k} - C_{3k})^2}\sqrt{f_{24}} \quad (18)$$

where: $$f_{24} = (C_{6k} - C_{1k})^2 (C_{6k} - C_{3k})^2 \delta Q_{12}^2 + Q_{12}^2 \left[(C_{6k} - C_{3k})^2 \delta C_{1k}^2 + (C_{6k} - C_{1k})^2 \delta C_{3k}^2 + (C_{1k} - C_{3k})^2 \delta C_{6k}^2\right] \quad (19)$$

Extract airflow rate $$\delta Q_{46} = T(P,\infty)\sqrt{\frac{(C_{62} - C_{42})^2 \delta I_2^2 + I_2^2(\delta C_{62}^2 + \delta C_{42}^2)}{(C_{62} - C_{42})^4}} \quad (20)$$

Recirculation flow rate $$\delta Q_{62} = \frac{T(P,\infty)}{(C_{6k} - C_{3k})^2}\sqrt{(C_{6k} - C_{3k})^2 (C_{3k} - C_{1k})^2 \delta Q_{12}^2 + Q_{12}^2 f_{62}} \quad (21)$$

where: $$f_{62} = (C_{6k} - C_{3k})^2 \delta C_{1k}^2 + (C_{6k} - C_{1k})^2 \delta C_{3k}^2 + (C_{3k} - C_{1k})^2 \delta C_{6k}^2$$

Alternatively $$\delta Q_{62} = \frac{T(P,\infty)}{(C_{6k} - C_{1k})^2}\sqrt{(C_{6k} - C_{1k})^2 (C_{3k} - C_{1k})^2 \delta Q_{24}^2 + Q_{24}^2 f'_{62}} \quad (22)$$

where: $$f'_{62} = (C_{6k} - C_{3k})^2 \delta C_{1k}^2 + (C_{6k} - C_{1k})^2 \delta C_{3k}^2 + (C_{3k} - C_{1k})^2 \delta C_{6k}^2$$

or if calculated from eq. (12): $$\delta Q_{62} = T(P,\infty)\sqrt{R^2 \delta Q_{24}^2 + Q_{24}^2 \delta R^2} \quad (23)$$

Infiltration: $$\delta Q_{04} = \frac{T(P,\infty)}{(C_{4k} - C_{0k})^2}\sqrt{(C_{3'k} - C_{4k})^2 (C_{4k} - C_{0k})^2 \delta Q_{24}^2 + Q_{24}^2 f'_{04}} \quad (24)$$

with $$f_{04} = (C_{3'k} - C_{4k})^2 \delta C_{0k}^2 + (C_{4k} - C_{0k})^2 \delta C_{3'k}^2 + (C_{3'k} + C_{0k})^2 \delta C_{4k}^2 \quad (25)$$

Exfiltration $$\delta Q_{40} = \sqrt{\delta Q_{04}^2 + \delta Q_{24}^2 + \delta Q_{46}^2} \quad (26)$$

Exhaust $$\delta Q_{60} = \sqrt{\delta Q_{04}^2 + \delta Q_{40}^2 + \delta Q_{01}^2} \quad (27)$$

2.2.3 Effect of large recirculation ratio on airflow rates confidence intervals

In equations (8), (10), and (13) the concentrations difference $C_{6k} - C_{3k}$ is at the denominator, and these two concentrations are close to each other at steady state when the recirculation ratio is high. This leads to a large confidence interval of the calculated airflow rates. In this case, it is better to inject the tracer gas at location 3 instead of location 2. The supply airflow rate can then be determined with a better accuracy, using:

$$Q_{24} = \frac{I_3}{C_{3'3} - C_{33}} \tag{28}$$

The confidence interval being calculated, *mutatis mutandis*, using equation (17) or, assuming that the confidence interval is the same for both concentrations:

$$\frac{\delta Q}{Q} \cong T(P,\infty)\sqrt{\left(\frac{\delta I}{I}\right)^2 + 2\left(\frac{\delta C}{C'-C}\right)^2} \tag{29}$$

The recirculation airflow rate can then be calculated using:

$$Q_{62} = Q_{24} - Q_{12} \tag{30}$$

with:
$$\delta Q_{62} = T(P,\infty)\sqrt{\delta Q_{24}^2 + \delta Q_{12}^2} \cong T(P,\infty)\sqrt{1+(1-R)^2}\ \delta Q \tag{31}$$

assuming that the relative error $\delta Q/Q$ is the same for both airflow rates, and taking into account that $Q_{12} = (1\text{-}R)\ Q_{24}$. Note that, in this case, δQ_{62} decreases when R increases.

The extract airflow rate Q_{46} cannot be assessed without injecting a tracer gas in the extract duct. However, in air handling units having no exhaust duct (such as most AHUs in Singapore and other tropical countries), $Q_{60} = 0$, hence $Q_{46} = Q_{62}$, and $Q_{40} = Q_{01} + Q_{04}$

2.2.4 Determining the optimum method for system with large recirculation ratio

The recirculation ratio is defined by:

$$R = \frac{Q_{62}}{Q_{24}} = \frac{Q_{62}}{Q_{62} + Q_{12}} \tag{32}$$

Assuming that there is no leak in the air handling unit, it can be assessed using:

Method **A**
$$R = \frac{C_{3k} - C_{1'k}}{C_{6k} - C_{1'k}} \tag{33}$$

the subscript k being for any tracer gas except the one injected in inlet duct. The confidence interval is:

$$\delta R = \frac{T(P,\infty)}{(C_{6k} - C_{1'k})^2}\sqrt{f_R} \tag{34}$$

where:
$$f_R = (C_{3k} - C_{6k})^2\,\delta C_{1'k}^2 + (C_{6k} - C_{1'k})^2\,\delta C_{3k}^2 + (C_{3k} - C_{1'k})^2\,\delta C_{6k}^2 \tag{35}$$

If we assume that the relative error is the same for all concentrations, and taking into account that, for tracers injected at locations 2 and 3, $C_{1'k} \cong 0$ and therefore $C_{3k} \cong R\ C_{6k}$, we can get a simpler expression for the confidence interval of the recirculation ratio:

$$\delta R \cong \frac{T(P,\infty)\ \delta C}{C}\sqrt{2(R^2 - R + 1)} \tag{36}$$

The recirculation ratio can also be calculated using:

Method **B** $R = \frac{Q_{62}}{Q_{24}}$ with $\delta R = \frac{\delta Q}{Q}\sqrt{(1+R)}$ (37)

Or Method **C** $R = 1 - \frac{Q_{12}}{Q_{24}}$ with $\delta R = \sqrt{2}\frac{\delta Q}{Q}(1-R)$ (38)

assuming that the relative error $\delta Q/Q$ is the same for both airflow rates, and taking into account that $Q_{12} = (1\text{-}R)\ Q_{24}$.

The three methods for determining R and δR are compared in Figure 2. Method A should be preferred at low recirculation ratio, while method C is best at large recirculation ratio. Method B could be applied at low recirculation if method A cannot be applied.

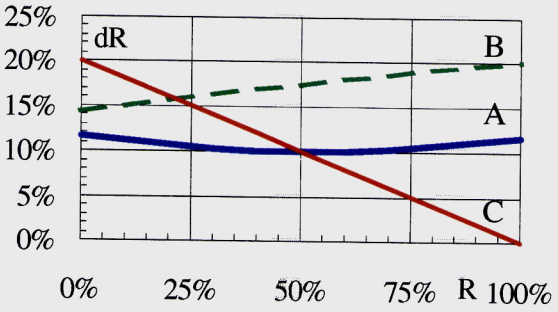

Figure 2: Confidence interval of the recirculation ratio as function of the recirculation ratio itself, for three assessment methods. For this figure, the relative confidence interval (at 90%) of injection rate and concentrations is 5%.

This error analysis shows that some method of conducting the measurement can provide more accurate results than others, and that the best way depends on the type of ventilation unit measured. Therefore, care should be taken to select the most appropriate method for large recirculation ratios. Measurement time could be shortened by fitting the dynamic expression of concentration on the experimental points to assess the steady state concentration without reaching it.

2.3 Measuring airflows in rooms with two air handling units

2.3.1 Modelling the airflow pattern

It is common in Singapore to find office spaces ventilated as shown in Figure 3. The full network corresponding to such a design is illustrated in Figure 4. The following symbols are applied in this figure:

o	outdoor air	i	infiltration air
s	supply air	e	exfiltration air
r	return air	BA	from AHU B to AHU A
x	extract air	AB	from AHU A to AHU B

Concentration of tracer gas should be measured in the room (node 2') to separately determine all illustrated airflow rates. This is not practical and may not be possible in many cases, since the building management may not allow drawing sampling tubes in the office rooms.

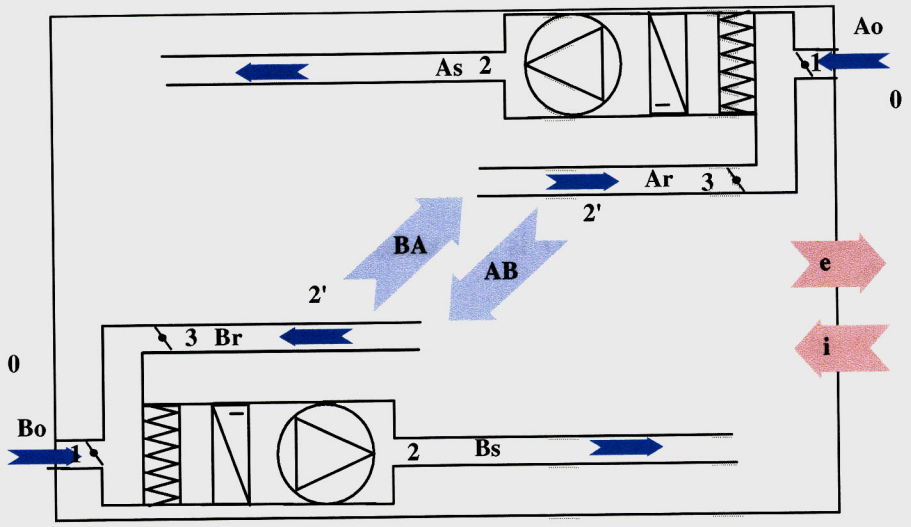

Figure 3: A room with two AHUs (A and B) with recirculation. Airflows are indicated by letters and network notes by numbers (see text)

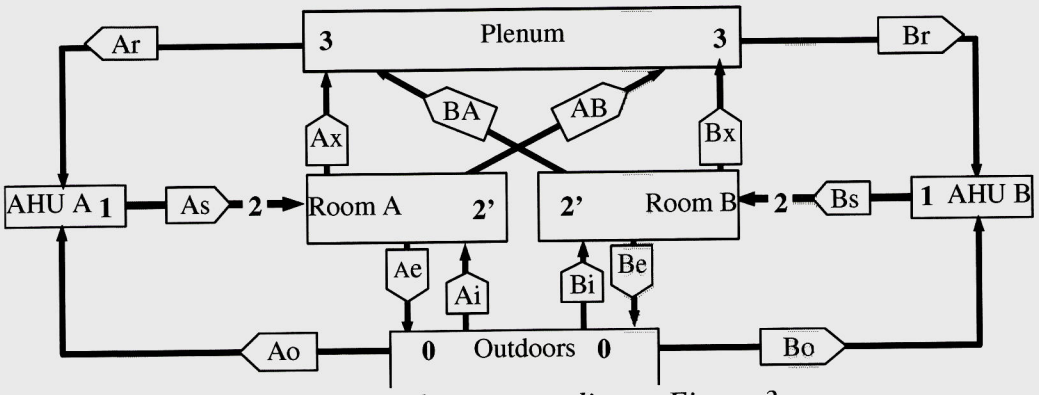

Figure 4: Complete equivalent network corresponding to Figure 3.

In order to allow determining the inter-AHUs airflow rates without sampling air in the room, the airflow pattern is modelled according to Figure 5..

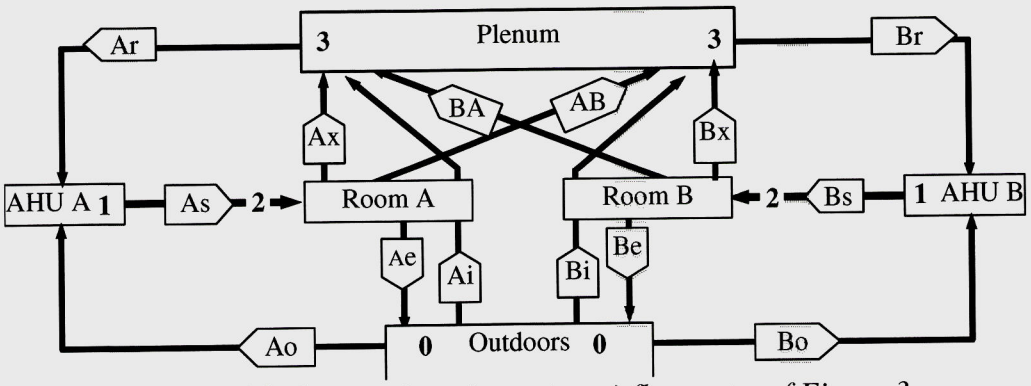

Figure 5: Proposed simplified network to determine airflow rates of Figure 3.

Nodes 2 are in the supply ducts. This supply air is assumed to go partly into both return ducts and to outside by exfiltration. Infiltration is assumed to dilute room air and ends into recirculation duct. This compromise does not allow the exact determination of infiltration in each separate room, and biases slightly the inter-AHU flow rates. It provides however an

estimate of these airflow rates, good enough in most cases, without having to sample air in the rooms. It takes account of the fact that a wall may separate rooms

Tracer gas 1 is injected into outdoor air duct, and tracer 2 into supply (either upstream the fan or in supply duct), once in AHU A, once in AHU B. There are hence either four tracer gases, or up to four successive experiments with the same tracer, assuming that airflow rates remain constant throughout the experiment.

Sampling points:
o outdoor air
i inlet duct, downstream the injection port of tracer 1,
1 after the supply fan, upstream the injection point of tracer 2,
2 supply duct, downstream enough to the injection port of tracer 2 to get good mixing,
3 return duct.

All sampling points are taken in both AHUs, *A* and *B*. For example, C_{iA1a} denotes the concentration of tracer 1 - injected in AHU A - in the inlet duct of AHU *A* downstream of the injection port of tracer gas.

2.3.2 Main airflow rates

Outdoor air and supply flow rates are obtained directly from concentrations of the tracer injected in inlet, respectively supply ducts and measurement of concentration upstream and downstream the injection locations:

$$Q_{Ao} = \frac{I_{1A}}{C_{iA1a} - C_{oA1a}} \quad \text{and} \quad Q_{Bo} = \frac{I_{1B}}{C_{iB1b} - C_{oB1b}} \tag{39}$$

$$Q_{As} = \frac{I_{2A}}{C_{1A2a} - C_{2A2a}} \quad \text{and} \quad Q_{Bs} = \frac{I_{2B}}{C_{1B2b} - C_{2B2b}} \tag{40}$$

Conservation of airflow rates in both AHUs provides the return airflow rates:

$$Q_{Ar} = Q_{As} - Q_{Ao} \quad \text{and} \quad Q_{Br} = Q_{Bs} - Q_{Bo} \tag{41}$$

Then, all main airflow rates can be assessed independently in each AHU, applying the method described in (Roulet and L.Vandaele 1991), and (Roulet, Deschamps et al. 2000). If measurements are performed in one AHU only, the outdoor air brought by the other AHU(s) is included in the infiltration flow rate.

2.3.3 Inter-units and leakage airflow rates

Applying air- and tracer mass conservation at node 3 provides two systems of three equations to obtain infiltration, extract and inter-AHUs airflow rates for both AHUs. Using a matrix notation, these are:

For AHU A

$$\begin{bmatrix} 1 & 1 & 1 \\ C_{oa} - C_{3Aa} & C_{2Aa} - C_{3Aa} & C_{2Ba} - C_{3Aa} \\ C_{ob} - C_{3Ab} & C_{2Ab} - C_{3Ab} & C_{2Bb} - C_{3Ab} \end{bmatrix} \begin{pmatrix} Q_{Ai} \\ Q_{Ax} \\ Q_{BA} \end{pmatrix} = \begin{pmatrix} Q_{Ar} \\ 0 \\ 0 \end{pmatrix} \tag{42}$$

Or

$$(\boldsymbol{C}_A)\vec{\boldsymbol{Q}}_A = \vec{\boldsymbol{Q}}_{Ar} \tag{43}$$

Similarly, for AHU B, we get, by permuting subscripts A and B:

$$(\boldsymbol{C}_B)\vec{\boldsymbol{Q}}_B = \vec{\boldsymbol{Q}}_{Br} \tag{44}$$

In these equations, tracer *a*, respectively *b* could be either the one injected in outdoor air inlet duct or into the supply air duct. Since the return airflow rates are known, these two systems can easily be solved:

$$\vec{\boldsymbol{Q}}_A = (\boldsymbol{C}_A)^{-1}\vec{\boldsymbol{Q}}_{Ar} \qquad \text{and} \qquad \vec{\boldsymbol{Q}}_B = (\boldsymbol{C}_B)^{-1}\vec{\boldsymbol{Q}}_{Br} \tag{45}$$

Exfiltration airflow rates are finally obtained by conservation of air at nodes 2A and 2B:

$$Q_{Ae} = Q_{As} - Q_{Ax} - Q_{AB} \qquad \text{and} \qquad Q_{Be} = Q_{Bs} - Q_{Bx} - Q_{BA} \tag{46}$$

Balance of whole rooms could be used for a check:

$$Q_{Ae} + Q_{Be} = Q_{Ao} + Q_{Bo} + Q_{Ai} + Q_{Bi} \tag{47}$$

2.3.4 Special case: No infiltration

If, from pressure differential measurements, it can be reasonably assumed that there is no infiltration, or if infiltration is negligible, the systems of equation (42) and (44) can be greatly simplified. For AHU A, for example:

$$\begin{aligned} &Q_{Ax} + Q_{AB} = Q_{As} \\ &Q_{Ax} + Q_{BA} = Q_{Ar} \\ &(C_{2Aa} - C_{3Aa})Q_{Ax} + (C_{2Ba} - C_{3Aa})Q_{BA} = 0 \\ &(C_{2Ab} - C_{3Ab})Q_{Ax} + (C_{2Bb} - C_{3Ab})Q_{BA} = 0 \end{aligned} \tag{48}$$

from which we can easily calculate the part of the return airflow rate that comes from AHU B:

$$\frac{Q_{BA}}{Q_{Ar}} = \frac{C_{2Aa} - C_{3Aa}}{C_{2Aa} - C_{2Ba}} = \frac{C_{2Ab} - C_{3Ab}}{C_{2Ab} - C_{2Bb}} \tag{49}$$

For AHU B, we get similarly:

$$\frac{Q_{AB}}{Q_{Br}} = \frac{C_{2Ba} - C_{3Ba}}{C_{2Ba} - C_{2Aa}} = \frac{C_{2Bb} - C_{3Bb}}{C_{2Bb} - C_{2Ab}} \tag{50}$$

Finally, the parts of the return airflow rate that comes from the same AHUs are:

$$\frac{Q_{Ax}}{Q_{Ar}} = 1 - \frac{Q_{BA}}{Q_{Ar}} \qquad \textit{and} \qquad \frac{Q_{Bx}}{Q_{Br}} = 1 - \frac{Q_{AB}}{Q_{Br}} \tag{51}$$

2.3.5 Special case: Perfect mixing

When complete mixing occurs in the rooms and/or plenum, the concentrations of all tracers do not differ significantly in both return ducts.

In this trivial case, both rooms and plenum can be combined in one single node, as shown in Figure 6. Only outdoor, supply and return airflow rates can be measured, since uncertainty on

concentration differences of equations (49) and (50) is too large. It can only be deduced, from the perfect mixing, that inter-room airflow rates are both much larger than supply or return airflow rates.

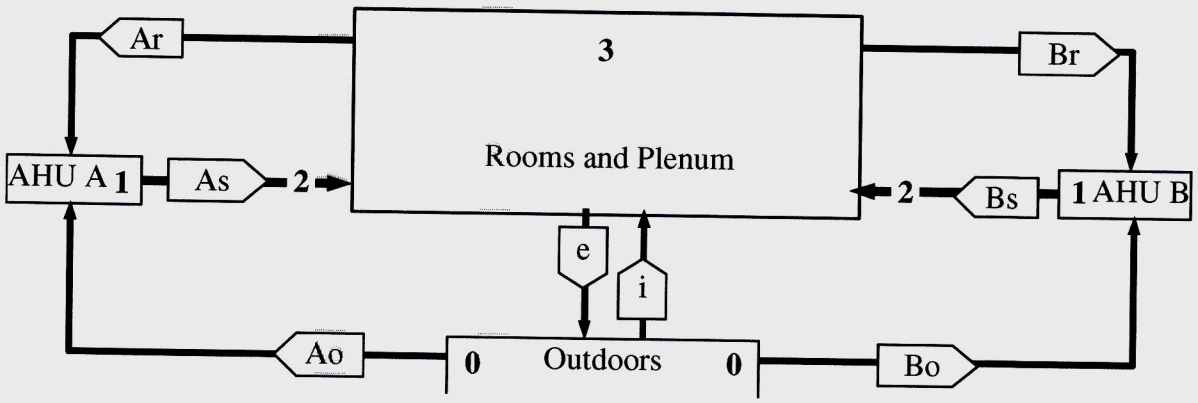

Figure 6: Simplest network corresponding to Figure 3 when perfect mixing occurs in the ventilated rooms.

2.3.6 Error Analysis

The accuracy of the result depends on the measurement conditions, in particular on the airflow rates themselves. Therefore, an error analysis is paramount to get some confidence in the results.

One of the ways to get the dispersion of the results caused by uncertainties in measured quantities (in this case tracer injection rates and concentrations) is to differentiate the equations of the interpretation algorithms, in order to get a relation linking the standard deviation of the results to the standard deviation of the input variables. This method is however practical only for the simplest cases. It is based on equation (16).(16)(16)

Then, the confidence interval of the outdoor airflow rate in AHU A given by equation (39) is:

$$\delta Q_{Ao} = T(P,\infty)\sqrt{\frac{\left(C_{iA1a}-C_{oA1a}\right)^2 \delta I_{1A}^2 + I_{1A}^2\left(\delta C_{iA1a}^2 + \delta C_{oA1a}^2\right)}{\left(C_{iA1a}-C_{oA1a}\right)^4}} \tag{52}$$

If the relative errors

$$\frac{\delta C}{C} \text{ and } \frac{\delta I}{I} \tag{53}$$

are the same for all concentrations and all injection rates, then:

$$\frac{\delta Q_{Ao}}{Q_{Ao}} = T(P,\infty)\sqrt{\frac{\delta I^2}{I^2} + 2\left(\frac{\left(C_{iA1a}+C_{oA1a}\right)}{\left(C_{iA1a}-C_{oA1a}\right)}\frac{\delta C}{C}\right)^2} \tag{54}$$

Confidence intervals for Q_{Bo}, Q_{As} and Q_{Bs} are obtained by similar formulas.

Then

$$\delta Q_{Ar} = \sqrt{\delta Q_{As}^2 + \delta Q_{Ao}^2} \tag{55}$$

and the same for δQ_{Br}.

If there is no infiltration, the confidence interval of the part of the return airflow rate in AHU A that comes from unit B is obtained by applying equation (14) to equation (11):

$$\delta\left(\frac{Q_{BA}}{Q_{Ar}}\right) = \frac{T(P,\infty)}{(C_{2Aa} - C_{2Ba})^2} f_R \tag{56}$$

where: $$f_R = (C_{3Aa} - C_{2Ba})^2 \delta C_{2Aa}^2 + (C_{2Aa} - C_{2Ba})^2 \delta C_{3Aa}^2 + (C_{2Aa} - C_{3Aa})^2 \delta C_{2Ba}^2 \tag{57}$$

A similar equation can be used for AHU B.

3 MATERIALS & METHODS

3.1 Case Study: description

Actual measurements were performed on the third floor of a newly commissioned (6 months old) 6-storey office building. A schematic plan of the building is presented in Figure 7.

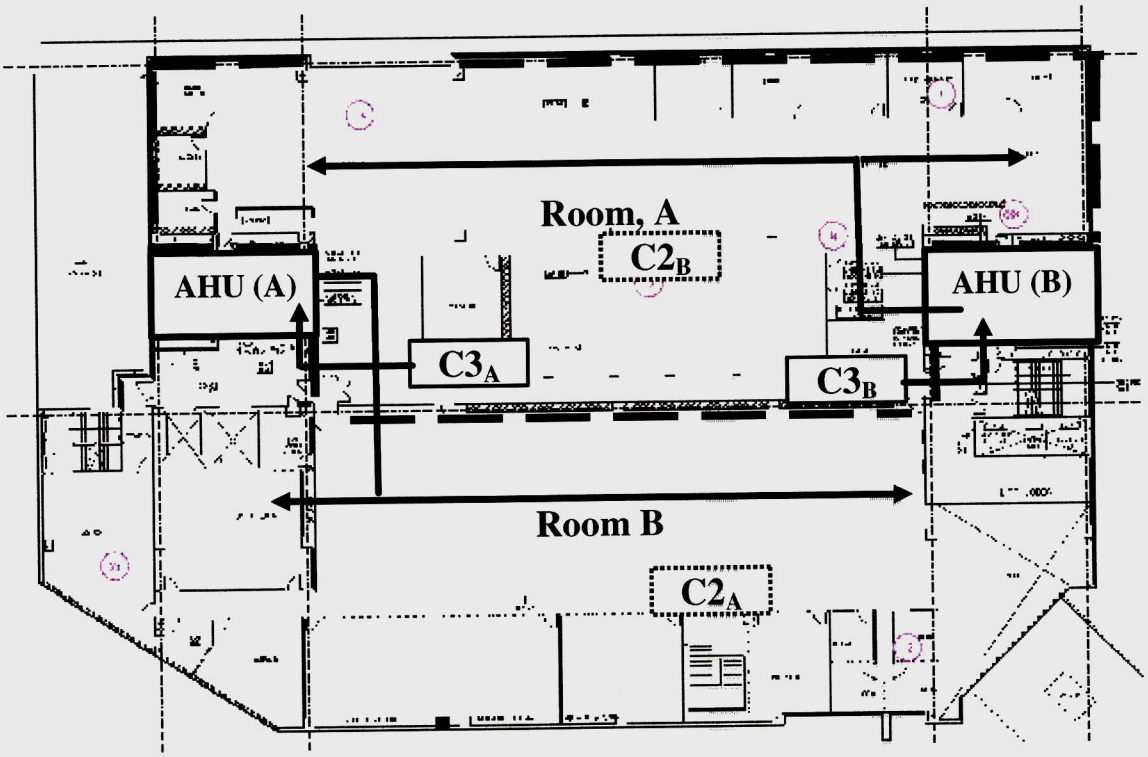

Figure 7: Layout of the measured space, showing the two air handling units and rooms for A and B. The arrows are schematic representation of the supply and return air ducts from the two AHUs. The locations of the rooms and return air sampling points are illustrated in the Figure. Locations of fresh air sampling points are in the respective AHUs.

It is a modern commercial office building with a very airtight design to reduce infiltration of unconditioned air. The space tested, which has an effective volume of 4,200m^3, is occupied by up to 70 people with about half the area installed with acoustic partitions. The floor is laid with polyester carpets and the activity observed was typical of an office environment. Ventilation in the indoor space is served by two separate air handling units. The office space can be divided into 2 large open office spaces separated by a high wooden cabinet. The arrows represent the position of the supply and return ducts for the 2 AHUs.

The air handling units, AHU (A) and AHU (B) that serve the space are located at the opposite sides of the building in two different AHU rooms. Outdoor air is provided via an internal airshaft drawing air from the roof of the building. A constant speed fan draws outdoor air via a short duct to each AHU room. This air is mixed with the space return air and blown through the filters and cooling coil of the AHU. From the AHU room, the main air supply duct distributing the conditioned air splits immediately into 2 main branches supplying various parts of the space via ceiling mounted diffusers. The distribution is by means of a variable air volume (VAV) system. However, for the experiment, the speed of the fan has been locked at a fixed frequency (50Hz) to facilitate measurements by preventing variations in the air flow rates due to the mechanisms of the VAV system. Return air is drawn from the main zone by way of grilles integrated with the suspended ceiling. The return air is drawn back to the AHU via the ceiling void, which acts as a return air plenum. There is no designed exhaust from the space, excess air leaves the space through exfiltration. In both AHUs, the units were equipped with new electrostatic air cleaners rated at 12 Pa pressure drop @ 1700 m^3/h (1000 cfm) mounted in a bank of 6 large and 3 smaller filters. The large and small filters have face areas of 500 X 800 mm^2 and 500 X 200 mm^2 respectively. The face velocity for the electrostatic filters was 1.75 ms^{-1}.

3.2 Instrumentation

The airflow rates in the building are determined by the constant injection technique using SF_6 as a single tracer gas. At the outset, it was decided to adopt method C (tracer gas injections in fresh air and supply ducts). This is based on the notion that the building adopts a large recirculating ventilation design and that method C provides the lowest associated airflow rates errors. Furthermore, the return air duct to the AHU is too short for tracer gas injection. In total, four successive tracer gas injections were performed. The tracer gas was injected in the fresh air and the supply air ducts at 10 mL/min and 280 mL/min respectively. These are optimal values calculated based on the design airflow rates of the fresh air and the supply air ducts and the desired concentration of tracer gas. The injection rate was maintained constant with the aid of a mass flow controller.

The concentrations of the tracer gas were sampled using polytetrafluoroethylene (PTFE) tubing. For upstream and downstream measurements, the PTFE tubes were inserted through drilled holes into the ducts. To determine cross-sectional average concentration uniformity of the tracer gas, multi-point samplings using the PTFE tubes were employed (Cheong, 1994). Room and return duct air were also sampled using the PTFE tubes. A multi channel sampler is used to draw the sampled air from various locations into a multi-gas monitor. There, the air samples are analysed with a photo acoustic infrared spectrometer.. When near steady state values have been reached, the dosing was stopped and the time recorded. Errors associated with instrumentation are estimated to 5% for both the mass flow controller and photo acoustic infrared spectrometer.

3.3 Theoretical and Experimental Fitting Evaluation

The correlation between theoretical (C_t) and measured (C_m) concentrations is statistically evaluated using techniques outlined by Hanna (1988). These techniques included residual analysis which allows a quantitative estimate of $(\overline{C}_t - \overline{C}_m)$ and correlation which allows a measure of agreement between theoretical and measured concentrations. Here, $\overline{C}_t$ is the mean of theoretical exponential concentrations, $\overline{C}_m$ is the mean of the experimentally measured concentrations. The correlation coefficient, R^2 is used as an index of agreement and the root mean square error (RMSE) to interpret the fittings accuracy. The value of RMSE should be minimised as close to zero as possible so that the theoretical equation is predicting at peak maximum accuracy. This is because a difference of zero should explain most of the variation in the measured values C_m. The RMSE is given as

$$RMSE = \sqrt{\frac{\sum_{i=1}^{n} \Sigma(C_{ti} - C_{mi})^2}{n}} \tag{58}$$

Hanna (1988) stated that the total fitting uncertainty can be defined as $\Sigma(C_t - C_m)^2$.

4 RESULTS

4.1 Concentration profiles – steady and unsteady state

For the fresh air duct measurements, it is observed that the steady state conditions for both AHUs can be easily achieved within a few minutes. Figure 8 illustrates the tracer gas concentration profiles upstream and downstream of the injection port in a fresh air duct. However, for the supply air duct measurements, steady state concentrations cannot be achieved even after eight hours. A typical upstream and downstream concentrations profile is given in Figure 9. Similarly, steady state concentrations in the two rooms and two return air ducts cannot be achieved (Figure 10). Indeed, the steady state conditions took a long time to reach due to the high recirculation and large nominal time constants. Therefore, the unsteady state method of determining the airflow rates was used.

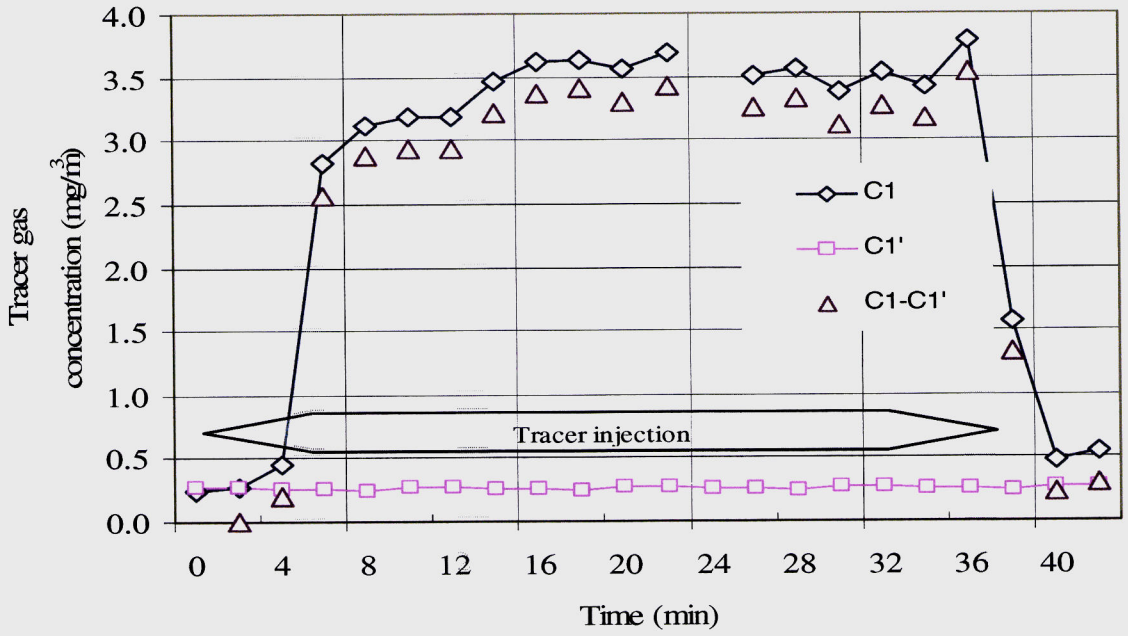

Figure 8: Tracer gas concentrations in fresh air duct, upstream (1) and downstream (1') the tracer gas injection port. (Dots are measured concentrations).

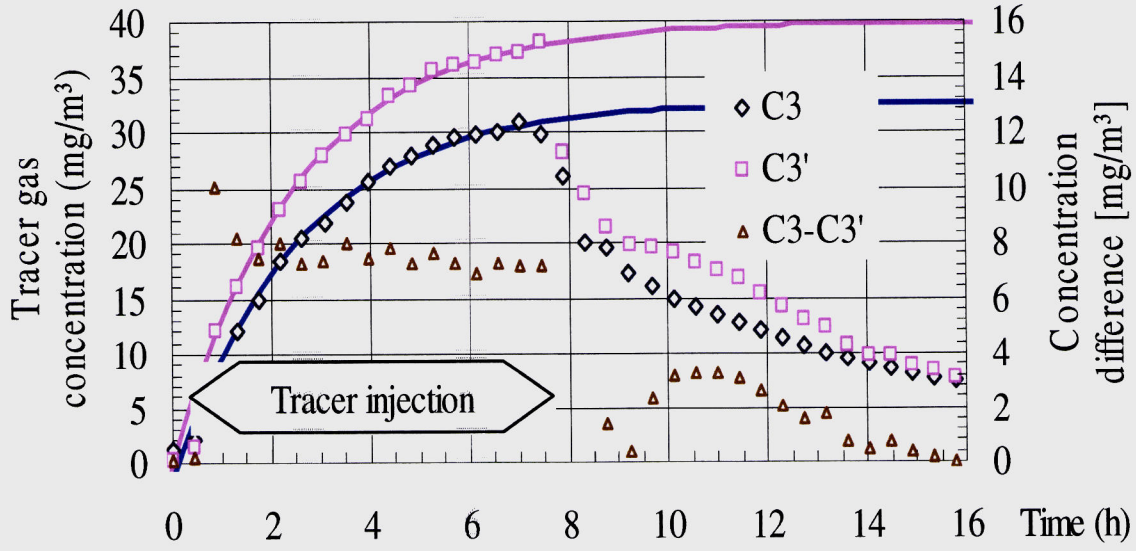

Figure 9: Tracer gas concentrations in supply duct, upstream (3) and downstream (3') the tracer gas injection port. Dots are measured concentrations, while lines are exponential fits.

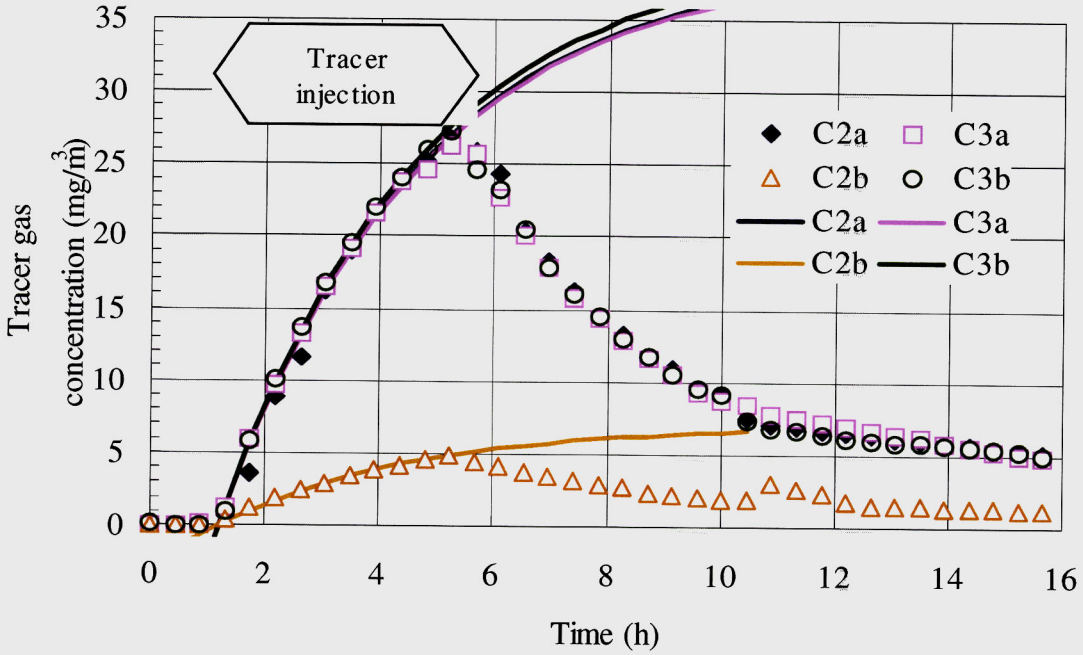

Figure 10: Tracer gas concentrations in two rooms (C2a and C2b) and return ducts (C3a and C3b). Dots are measured concentrations, while lines are exponential fits.

Based on the four successive tracer gas injections performed in the case study building, the experimental and theoretical steady state concentrations are tabulated (see Table 1). Since steady state concentrations can be achieved in the fresh air duct measurements, the average experimental concentrations were given. The remaining steady state concentrations were derived from the theoretical exponential fittings using equation 6. The room and return duct steady state concentrations were obtained with injection 3.

Table 1: Steady state concentrations determined from measurements in case study building.

Sampling locations			Steady state concentrations (mg/m^3)			
			Injection No	Average value	Standard Deviation	Source
Fresh air duct (A)	Downstream,	C_{iA1a}	1	3.5	1.4	Measured
	Upstream,	C_{oA1a}		0.3	0.1	Measured
Fresh air duct (B)	Downstream,	C_{iB1b}	2	3.5	1.4	Measured
	Upstream,	C_{oB1b}		0.3	0.1	Measured
Supply air duct (A)	Downstream,	C_{1A2a}	3	36.4	0.7	Extrapol.
	Upstream,	C_{2A2a}		26.7	1.4	Extrapol.
Supply air duct (B)	Downstream,	C_{1B2b}	4	31.5	4.8	Extrapol.
	Upstream,	C_{2B2b}		26.3	0.4	Extrapol.
Room (A),		C_{2a}	3	39.5	0.5	Extrapol.
Room (B),		C_{2b}	3	7.1	0.1	Extrapol.
Return air duct (A),		C_{3a}	3	39.3	0.8	Extrapol.
Return air duct (B),		C_{3b}	3	40.4	0.4	Extrapol.

The extrapolation model is statistically evaluated according to the ASTM standard guide D5157-97 (ASTM 1997). Resulting statistics are presented in Table 2. Intercept and slope are the coefficient of the regression line between calculated and measured values. The intercepts

are very small when compared to the concentrations, and the slopes are very close to 1, except for C_{2A2}. Correlations coefficients of this regression line are also very close to 1. The normalised mean square error (*NMSE*), a measure of the magnitude of the prediction error is close to zero, as is the normalised fractional bias FB_{50} of the mean concentrations for the highest half of observed concentrations.

Table 2: Quantitative measures of fitting performance between theoretical and measured concentrations.

	Intercept	Slope	*r*	*NMSE*	FB_{50}
C_{2a}	1,37	0,94	0,998	0,0030	0,0001
C_{3a}	-0,36	1,02	0,999	0,0005	0,0034
C_{2b}	-0,31	1,07	1,000	0,0022	0,0015
C_{3b}	-0,04	1,00	1,000	0,0002	0,0008
C_{1A2}	-2,72	1,10	0,995	0,0020	0,0081
C_{2A2}	4,96	0,79	0,990	0,0183	0,0022
C_{1B2}	-1,10	1,10	0,999	0,0003	0,0149
C_{2B2}	-2,11	1,19	0,997	0,0063	-0,0240

Overall, this analysis shows that the model used to extrapolate the concentrations predicts accurately the measured concentrations..

4.2 Calculated airflow rates

The results of the airflow rates measurements using the above model are shown in Table 3:. Only significant digits are provided. Therefore, a small airflow rate not significantly different from zero is shown as zero.

The results show that the supply air from both AHUs are not balanced. The main airflow rate in AHU B is almost the double of that in AHU A. Similarly, the return air flow rate in AHU B is twice that of AHU A. The airflow rate from room A to room B is much larger than the flow rate from the reverse direction. On the contrary, extract air from room A into unit A is large and the corresponding flow rate is not significant in room B. The recirculation ratios for both AHUs are very high.

Table 3:: Airflow rates determined from measurements in case study building..

		Airflow rates in m^3/h.	
		AHU A	AHU B
Outdoor air	*o*	900 ±200	900 ±200
Supply	*s*	17000 ±2'000	33000 ±5'000
Return	*r*	16000 ±2'000	32000 ±5'000
Recirculation ratio	*R*	95 ±1%	97 ±1%
From other room		100 ±900	33000 ±5'000
Extract same room	*x*	16000 ±2'000	0 ±7'000

5 Discussion

The dynamic fitting of theoretical exponential on the experimental points in Figure 9 and Figure 10 suggests that measurement time can be shortened without reaching steady state concentration. Indeed, the good statistical agreement between the two supports this notion.

However, it does not encourage limited readings to be taken as this would increase the extrapolation errors. Certainly, the measurement time should be large enough for sufficient accuracy to be achieved, since measured and theoretical concentrations tend to be closer as time progresses. The cumulative total fitting errors $\Sigma(C_t - C_m)^2$ associated with the difference between the theoretical exponential and experimental concentrations for different time intervals are tabulated (Table 4) to illustrate this point. In general, it is observed that the errors are rather large in the first hours and diminishes as time passes. In the example given in Figure 9, the effective time constant was τ = 2,5 hours. Therefore, based on the tabulated errors given, a minimum of two nominal time constant is preferred.

Table 4: Cumulative total fitting uncertainties $\Sigma(C_t - C_m)^2$ for different time intervals

	Time intervals			
$\Sigma(C_t - C_m)^2$	1–2 hr	2-3 hr	3-4 hr	4-5 hr
C_{2a}	4.38	6.53	0.00	0.16
C_{3a}	0.10	0.04	0.01	0.49
C_{2b}	0.13	0.04	0.00	0.00
C_{3b}	0.09	0.09	0.00	0.15
C_{1A2a}	7.71	0.06	1.50	0.45
C_{2A2a}	17.54	20.50	2.45	1.71
C_{1B2b}	7.84	0.48	0.55	0.47
C_{2B}	0.72	0.42	1.43	0.34
mean	4.81	3.52	0.74	0.47

This example illustrates the fact often observed that the most appropriate measurement and interpretation method depends in the situation. Looking at equations (15) to (19), it is obvious that the tracer gas injection and air analysis locations should be chosen in such a way that the concentration differences appearing either in these equations or in the matrix of equation (4) should be as large as possible. Another way of improving the accuracy of the results is to choose, among the several possible interpretations, the one leading as directly as possible to the results, with the minimum number of mathematical operation, since each operation may increase the confidence interval of the result.

6 CONCLUSIONS

It is shown that the tracer gas method used for assessing airflow rates in air handling units can easily be extended to two - or even more - units, provided that tracer gas experiments are performed in all units. Such measurements could be useful to explain the transfer of pollutants from one location to another in the space, or to check the balance of the airflow rates provided by several units ventilating the same space.

ACKNOWLEDGEMENTS

The National University of Singapore hosted C.-A. Roulet as Visiting Senior Research Fellow for three months. The starting idea of this paper, and the improved collaboration between NUS and EPFL building departments that made this development possible, result from this visit. The authors also like to thank A. Ranjith for helping in the measurements.

REFERENCES

ASHRAE (1999). *ASHRAE Handbook. HVAC Applications*. American Society of Heating, Refrigerating and Air-Conditioning Engineers, Atlanta, USA.

ASTM (1988). ASTM E 741-83: Standard Test Method for Determination of Air Leakage Rate by Tracer Dilution. *Annual Book of Standards*. ASTM. Philadelphia, PA, ASTM..

ASTM (1997). Standard Guide for Statistical Evaluation of Indoor Air Quality Models. West Conahoken, Pa, US, ASTM: 4.

Presser, K. H. and R. Becker (1988). "Mit Lachgas dem Luftstrom auf der Spur Luftstrommessung in Raumlufttechnischen Anlagen mit Hilfe der Spurgasmethode." *Heizung Luftung Haustechnik* 39(1): 7-14.

Roulet, C.-A., L. Deschamps, et al. (2000). DAHU: Diagnosis of Air Handling Units. *Air Distribution in Rooms - Ventilation for Health and Sustainable Development.* H. B. Awbi, ed.. Reading, UK, Elsevier. Vol 2: 861-866.

Roulet, C.-A., F. Foradini, et al. (1994). Use of Tracer Gas for Diagnostic of Ventilation Systems. *Healthy Buildings'94*, Budapest.

Roulet, C.-A. and L.Vandaele (1991). *Airflow Patterns within Buildings - Measurement Techniques*. AIVC, Bracknell. Order at inive@bbri.be.

Simons MW and Walters JR (1998). Local Ventilation Effectiveness Parameters in Air Distributon System Design Building *Services Engineering Research and Technology*, 19, (3), 135-140.

LIST OF FIGURES

LIST OF TABLES